Biosensors and Bioelectronics 132 (2019) 326–332

Contents lists available at ScienceDirect

Biosensors and Bioelectronics

journal homepage: www.elsevier.com/locate/bios

New strategy for the gene mutation identification using surface enhanced Raman spectroscopy (SERS)

Agata Kowalczyk[a], Jan Krajczewski[a], Artur Kowalik[b], Jan L. Weyher[c], Igor Dzięcielewski[c], Małgorzata Chłopek[b], Stanisław Góźdź[b], Anna M. Nowicka[a,*], Andrzej Kudelski[a]

[a] Faculty of Chemistry, University of Warsaw, Pasteura 1 Str., PL 02-093 Warsaw, Poland
[b] Holy Cross Cancer Center, Stefana Artwińskiego Str. 3, PL 25-734 Kielce, Poland
[c] Institute of High Pressure Physics of the Polish Academy of Science, Sokolowska 29/37 Str., PL 01-142 Warsaw, Poland

ARTICLE INFO

Keywords:
Conformation analysis
DNA recognition
Gene mutation identification
SERS
Surface analysis

ABSTRACT

An early and accurate diagnosis of a specific DNA mutations has a decisive role for effective treatment. Especially, when an immediate decision on treatment most needs to be made, the rapid and precise confirmation of clinical findings is vital. Herein, we show a new strategy for the gene mutation (BRAF c.1799T > A; p. V600E) identification using highly SERS-active and reproducible SERS substrate (photo-etched GaN covered with a thin layer of sputtered gold) and surface enhanced Raman scattering (SERS) spectroscopy. The detection is based on the conformation change (*gauche* → *trans*) of the alkanethiol linker modifying the capture DNA during the hybridization process. The value of the intensity ratio of the ν(C–S) bands of the *trans* and *gauche* conformer higher than 1.0 indicated the presence of mutation. The demonstrated new DNA SERS (bio)sensor is characterized by the low detection limit at the level of pg μL^{-1}, wide analytical range from 6.75 pg μL^{-1} to 67.5 ng μL^{-1} and high selectivity. The proposed bioactive platforms, based on nanostructured GaN substrates modified with thiolated ssDNA (single stranded DNA) can be successfully used in the analysis of clinical samples.

1. Introduction

Over the last decade, we have witnessed the tremendous advances in next generation diagnostics which are a result of developments in modern nanotechnology (Chertow, 2018; Heath, 2015; Jabir et al., 2012). The rapid detection of gene mutation, tumor cells or other cancer biomarkers, which facilitates better disease diagnosis, monitoring and management is especially a major challenge in the field of personalized medicine, matching patient's needs with appropriate therapeutic strategies that improve the health outcomes due to proper treatments. Among oncological patients 90% of deaths are due to metastatic cancer (Torre et al., 2015). In the case of solid tumors (lung cancer, colorectal cancer, breast cancer and melanoma) not infrequently there are difficulties in obtaining diagnostic material. Therefore, it is necessary to search for other sources of material that would be easily collected, provide diagnostic data to regularly monitor the effectiveness of treatment. A material with such features is peripheral blood, which reaches all the cells of the body (Pantel et al., 2009). The tumor releases in the bloodstream tumor cells (CTCs) and nucleic acids (circulating free tumor nucleic acids – ctNA), which are currently being attempted to adapt to diagnostics in the form of so–called a liquid biopsy (Khetrapal et al., 2018; Pérez-Barrios et al., 2016). The source of circulating tumor DNA (ctDNA) are cancer cells that undergo apoptosis (Crowley et al., 2013; Schwarzenbach et al., 2011). ctDNA released from cancer cells is usually fragmented and has a short length of about 100–200 bp (Diehl et al., 2005; Mouliere et al., 2011). ctDNA represents 1.4–47.9% of circulating free nucleic acids (cfNA) in the blood circulation of oncological patients (Leary et al., 2012). ctDNA is present in 50–75% of patients with advanced as well as localized cancer *e.g.* pancreatic, breast, intestine, kidney and brain cancers (Bettegowda et al., 2014).

Circulating free tumor deoxyribonucleic acid (ctDNA) is detected and tracked primarily based on tumor–related genetic and epigenetic alterations (Han et al., 2017). The possibility of using ctDNA to detect mutations in genes of predictive and prognostic importance for molecularly targeted therapies has been demonstrated (Oellerich et al., 2017). A big advantage of ctDNA analysis is the possibility of earlier – up to 10 months – detection of disease progression in comparison with radiological methods (Oellerich et al., 2017). The problem in using ctDNA for diagnostics is the scarce amount of material released into the bloodstream and the lack of ultra–sensitive diagnostic methods capable of detecting 0.1–0.01% of the mutated allele.

* Corresponding author.
E-mail address: anowicka@chem.uw.edu.pl (A.M. Nowicka).

https://doi.org/10.1016/j.bios.2019.03.019
Received 8 February 2019; Received in revised form 8 March 2019; Accepted 11 March 2019
Available online 12 March 2019
0956-5663/

In the early stages of the cancer, only trace levels of biomarkers exist, so they should be detected with high sensitivity and minimally invasive medical procedures. Currently, the clinical cancer identification is mainly done using imaging techniques, such as X–ray, mammography, computed tomography, magnetic resonance imaging, endoscopy and ultrasonography. Unfortunately, their usefulness in distinguishing between benign and malignant changes is limited (Chinen et al., 2015). The existing genomic and proteomic protocols for ctDNA determination in some body fluids and/or tissues are time consuming. In consequence, the risk of patients spreading disease whilst awaiting results increases. Therefore a non–invasive, selective, ultrasensitive and rapid protocols for early stages of cancer identification are still needed. Surface–enhanced Raman scattering (SERS) fulfills those expectations very well. It is one of the ultrasensitive methods, which can be used for characterization at the molecular level (Chen et al., 2013; Wu et al., 2015; Zhang et al., 2018). SERS can provide specific spectroscopic fingerprints of biomolecular structures and compositions of tissues, therefore it is a promising technique for the detection and identification of circulating tumor cells. Up to now various approaches for SERS sensors for the detection of the specific DNA fragments have been developed (Wang et al., 2010, 2013a) based on: (i) Raman reporter connected to the complementary single stranded DNA – after hybridization Raman reporter is moved close to the plasmonic nanostructure and a strong SERS signal is recorded (Cao et al., 2002; Fabris et al., 2007; Gao et al., 2013; Huang et al., 2015; Peng et al., 2014; Vo-Dinh et al., 2002), (ii) the sensor is composed of a DNA hairpin chain and a SERS-active plasmonic structure, one end of the hairpin probe is covalently bonded to the plasmonic structure, and the other is tagged with a Raman reporter, in the presence of the specific DNA target, hybridization between the target and DNA probe disrupts the stem-loop configuration and spatially separates the Raman reporter from the surface of the plasmonic structure which causes decrease in the measured SERS signal of the Raman reporter (Wang and Vo-Dinh, 2009; Wang et al., 2013b), (iii) formation of the sandwich-type structures due to the DNA hybridization reaction and immobilization of plasmonic nanoparticles or plasmonic nanoparticles with attached Raman reporters on various substrates (Chen et al., 2014; Fu et al., 2016) including magnetic nanoparticles (Yu et al., 2017) (iv) aggregation of the plasmonic nanoparticles induced by target DNA – presence of the specific DNA target cases aggregation of the plasmonic molecules and a significant increase in the intensity of the measured SERS spectrum, (Wang et al., 2017; Xu et al., 2018), (v) SERS signal of the specific nucleobases normalized to the signal of the phosphate backbone (Xu et al., 2015), (vi) the detection of point mutations in large DNA fragments utilizing the single-strand conformation polymorphism technique, utilizing the observation of the large conformational changes that single- and multiple-base substitutions impose on long single-stranded chains (Morla-Folch et al., 2017).

In this work we show a new strategy for identification of ctDNA using SERS spectroscopy. In our approach the modified at 5′ end with the hexanethiol linker ssDNA strands, complementary to the target ssDNA, were self–assembled on the highly SERS–active substrate. The recognition layer formed in this way was able to react with the analyte (target DNA). We found that the conformation of the hexanethiol linker, *via* which the capture ssDNA is attached to the gold surface, depends on the presence of the ssDNA fragments complementary to the immobilized strands in the analyzed sample. In the presence of the complementary ssDNA fragments the relative surface concentration of the hexanethiol moieties having the *trans* conformation of the Au–S–C–C chains is significantly higher than when only non–complementary ssDNA strands are present in the analyzed sample. It means that to identify a given ssDNA strand (and hence to identify the DNA mutation), one can use the phenomenon of the hybridization process changing the conformation (*gauche–trans*) of the thiol chain *via* which probe DNA strands are attached to the metal surface. One of the most frequently mutated proteins in the MAPK pathway is the *BRAF* protein. In most cases, the mutation c.1799T > A (p. V600E) is detected (Davies et al., 2002). The gene coding for the BRAF protein is mutated in 40–70% of papillary thyroid cancers, 50% of melanomas and about 10–20% of colon cancers (Domagała and Kowalik, 2014; Hodis et al., 2012; Kowalik et al., 2017; Rutkowski et al., 2014). Therefore, we decided to practically test our new approach for identification of a gene mutation (BRAF c.1799T > A; p. V600E) in clinical samples isolated from tissues and plasma of patients with papillary thyroid carcinoma and melanoma.

2. Experimental setup

2.1. Materials

All chemicals were of the highest purity available. Sodium acetate (NaAc; p.a., POCH, Poland), tris(2–carboxyethyl)phosphine hydrochloride (TCEP; Sigma), magnesium acetate ($Mg(Ac)_2$; p.a., POCH, Poland), 2–amino–2–(hydroxymethyl)propane–1,3–diol (Tris; Sigma), EDTA (Sigma), absolute ethanol (99.8%; POCH, Poland), 1–propanethiol (HS–C_3H_7, Sigma), 4–mercaptobenzoic acid (HS–C_6H_4COOH, Sigma), 6–mercaptohexan–1–ol (MCH; Sigma). All oligonucleotides were purchased from MWG–Operon (Eurofins). The following oligonucleotide sequences were used:

- probe DNA (5′→3′): thiol–C_6–CTAGCTACAGAGAAATCTCGAT,
- complementary target DNA (5′→3′): ATCGAGATTTCTCTGTAGC TAG,
- non–complementary DNA (5′→3′): GCTTGACCGGACTGTCCAAGGT

Thiols are strong nucleophiles and unprotected thiols spontaneously form disulphides in neutral aqueous solution, therefore the thiolated DNA fragments are synthesized as a disulfide. For reducing the disulfide bond of thiol–modified oligonucleotides to the active sulfhydryl form the probe DNA was dissolved in 200 µL of 10 mM TCEP in TE buffer (10 mM Tris, 1 mM EDTA, pH 8.0). Then, the solution was mixed in ThermoMixer (Eppendorf) for 60 min at room temperature. Next, the 150 µL solution containing 0.3 mol of NaAc and 1 mmole of $Mg(Ac)_2$ was added to the mixture. The tube was fill with absolute ethanol, gently shaked and incubated for 20 min at −20 °C. To isolate the obtained precipitate (HS–DNA) from the mixture the solution was centrifuged at 13,000 rpm for 5 min. At the end the pellet was dried at room temperature.

2.2. Clinical samples

The study material consisted of DNA isolated from FFPE tumor tissue and plasma collected from papillary thyroid carcinoma cases and cases of malignant melanoma. Isolation was performed using the Maxwell® 16 FFPE Plus LEV DNA Purification Kit (Promega) and Maxwell® RSC ccfDNA Plasma Kit (Promega) according to the manufacturer's recommendations. *BRAF* p. V600E mutation was detected using the Bio–Rad QX100 droplet digital PCR (ddPCR) platform. Samples preparation were performed according to manufacturer instruction using Droplet PCR Supermix for Probes (No dUTP) (Bio–Rad), wild type primers/probe assay (PrimePCR™ ddPCR™ Mutation Assay: *BRAF* WT for p. V600E, HEX, Bio–Rad) and mutation primers/probe assay (PrimePCR™ ddPCR™ Mutation Assay: *BRAF* p. V600E, FAM, Bio–Rad). The concentration of DNA isolates plasma and tissue ranged from 0.1 to 0.5 and 30–50 ng μL^{-1}, respectively. It should be stressed that the number of base pairs in the clinical samples was at least 10–fold higher than in the synthetic (target ssDNA).

2.3. Modification of the SERS substrate with DNA fragments

SERS platforms used in this study were fabricated by nano–structuring of hetero–epitaxial Si–doped n–type GaN on sapphire

samples, with free carrier concentration of $n = 1{\cdot}10^{18}$ cm^{-3}. The samples were photo–etched in a 0.02 M $K_2S_2O_8$ + 0.02 M KOH solution (designated KSO–D in ref. (Weyher et al., 2002)) under a 300 W UV–enhanced Xe lamp (Oriel) illumination in galvanic mode. This procedure was found to be optimal for high enhancement of SERS signal from the test pMBA analyte (Weyher et al., 2019). The surface morphology of the photo–etched samples was examined in scanning electron microscope (SEM Zeiss Ultra Plus). After etching, thin layer of gold was sputtered using a Quorum Q150TS sputter coater with a function of cleaning oxidized targets. Before SERS measurements the samples were cleaned using argon plasma function in Quorum Q150RS sputterer.

To modify the SERS substrate by the single– and double stranded DNA fragments the following procedure was applied. First, the DNA solutions (400 ng μL^{-1} in water) were heated for 10 min at the DNA melting temperature specified by the manufacturer to protect the single stranded DNA fragments from interactions with each other. Next, the solutions were immediately cooled down in the ice bath and diluted with distillated water (Hydrolab, conductivity 0.056 $\mu S\ cm^{-1}$). Next, the 20 µL droplet of probe DNA (69.1 ng μL^{-1}) was placed at the gold substrate and left under the cover for 2 h at room temperature. The substrate with self–assembled thiol DNA fragments was carefully rinsed with water to remove non–adsorbed thiol DNA molecules. To prevent the irregular adsorption of nucleic bases at the SERS substrate and simply makes the layer uniform (Levicky et al., 1998), the substrate modified with self–assembled probe DNA was immersed in 1 mM MCH aqueous solution. After 1 h the substrate was removed from MCH solution and gently washed with water. The hybridization process was performed at 36 °C by introduction of 20 µL droplet containing 67.5 ng μL^{-1} of complementary target ssDNA on the substrate modified with thiolated probe DNA/MCH and left under the cover for 60 min. The same procedure was applied in the case of natural samples. The scheme of the SERS substrate modification procedure is presented in Scheme 1A.

2.4. SERS investigations

SERS spectra were recorded using a Horiba Jobin–Yvon Labram HR800 spectrometer connected to an Olympus BX40 confocal optical microscope equipped with a 50 × long distance objective. Raman spectrometer was equipped with a diode laser emitting at 785 nm, a 600 grooves/mm holographic grating, and a Peltier–cooled CCD detector (1024 × 256 pixel). The SERS substrates modified with a chemisorbed capture ssDNA were immersed in the analyzed solution of DNA, and the SERS spectra were collected for SERS substrates being covered with the analyzed solution.

3. Results and discussions

3.1. GaN substrate characteristics

The quality of the measured SERS spectra is strongly dependent on the SERS–activity of the used plasmonic substrate and its reproducibility. Therefore, to carry out these DNA SERS studies we used one of the most reproducible SERS substrates described in the literature – photo–etched GaN covered with the layer of gold (Kaminska et al., 2011). The SERS materials produced by the deposition of films of plasmonic metals on nanostructured surfaces (as nanostructured surface of GaN) are excellent substrates for SERS measurements (Lai et al., 2014). The nano–structures of GaN after photo–etching is shown in Fig. 1A. The nano–pillars in Fig. 1 were formed on dislocations due to effective recombination of photo–carriers along the linear defects. This effect was well recognized and was discussed in refs (van Dorp et al., 2009; Weyher and Macht, 2004; Weyher et al., 2001). The surface morphology of photo–etched and of Au–coated samples is shown in Fig. 1A and B-C, respectively. The high magnification image of the bunch termination of nano–pillars (see Fig. 1C) shows that after sputtering the plazmonic metal layer is not continuous, but consists of Au nano–clusters of less than 100 nm size. The nanostructure nature of the GaN substrates allow to use them as a stable, reproducible and highly active SERS platforms. The detailed characterization of this SERS substrate is presented in our previous work (Weyher et al., 2019). The average SERS enhancement factor achieved on this substrate was determined as equal to *ca.* $2.1{\cdot}10^6$ (Weyher et al., 2019).

3.2. DNA–hybridization biosensor with SERS monitoring

In our approach the GaN substrate for surface–enhanced Raman scattering experiments, modified with the self–assembled DNA monolayer was used for search of the gene mutation. To obtain the information about the amount of thiolated DNA fragments introduced on the SERS substrate *via* Au–S bond the UV–vis spectra of the solutions containing probe DNA before and after immobilization step were recorded, see Fig. 2. From the difference of the obtained absorbance value at the DNA band (*ca.* 260 nm), the number of DNA fragments immobilized on the SERS substrate was calculated. The surface concentration of probe DNA on the SERS substrate (5 × 5 mm) was calculated as 1.38 µg cm^{-2}. To check the ability of the self–assembled thiolated DNA to the hybridization process the absorbance changes of the solution containing synthetic complementary target DNA was monitored (Fig. 2). On the basis of the decrease in the intensity of the absorption band of target DNA, before and after interaction with probe DNA, its surface concentration was determined to be 1.21 µg cm^{-2}. It indicates that almost every immobilized probe DNA fragment is capable to taking part in the hybridization process, the efficiency of this process is equal 90%.

Detection of the hybridization process was performed using surface enhanced Raman spectroscopy. Fig. 3 illustrates the representative SERS spectra of GaN substrates modified with ssDNA before (blue line, Fig. 3A-C) and after hybridization process with synthetic target DNA – fully complementary (red line, Fig. 3A-B), non–complementary DNA (green line, Fig. 3C) and DNA isolated from FFPE tumor tissue with *BRAF* c.1799T > A; p. V600E mutation (Fig. 3A) collected from papillary thyroid carcinoma cases and cases of malignant melanoma and plasma without *BRAF* mutation (Fig. 3B).

The most characteristic Raman bands, which appear in the analyzed wavenumber region (marked in Fig. 3) are bands near 700 cm^{-1} (at 640 cm^{-1} and at 714 cm^{-1}). These bands are due to the ν(C–S) stretching vibration of the alkanethiols adsorbed on the gold surface. The ν(C–S) band at a lower wavenumber (640 cm^{-1}) is characteristic for molecules having the *gauche* conformation of the Au–S–C–C chain (see Scheme 1B), whereas the $\nu(C-S)$ band at a higher wavenumber (714 cm^{-1}) is characteristic for molecules having the *trans* conformation of the Au–S–C–C chain, see Scheme 1B (Bryant and Pemberton, 1991a, 1991b; Kudelski, 2003; Tarabara et al., 1998). Both bands are shifted toward lower wavenumbers in comparison to that of the liquid hexanethiol at 657 and 738 cm^{-1}. This shift can be related to a withdrawal of electron density from the C–S bond because of bonding of the sulphur atom to gold (Bryant and Pemberton, 1991a; Kudelski and Hill, 1999). Although the Au–S–C–C fragment of the chemisorbed thiol–modified DNA is only a very small part of the whole adsorbed system, the vibrations localized at that part of the molecule that directly interacts with the gold substrate can dominate the measured SERS spectrum because the SERS enhancement factor decrease significantly with the increasing distance from the surface of the plasmonic nanostructure (one can predict the r^{-10} distance dependence of the SERS enhancement factor) (Kennedy et al., 1999; Stiles et al., 2008).

As can be seen in Fig. 3A, in the case of the presence at the GaN substrate only the probe DNA sequence the intensity ratio of the ν(C–S) bands of the *trans* and *gauche* conformer was equalled about 0.9. After hybridization with the complementary synthetic ssDNA strands (target DNA, red line in Fig. 3A) or with DNA isolated from FFPE tumor tissue

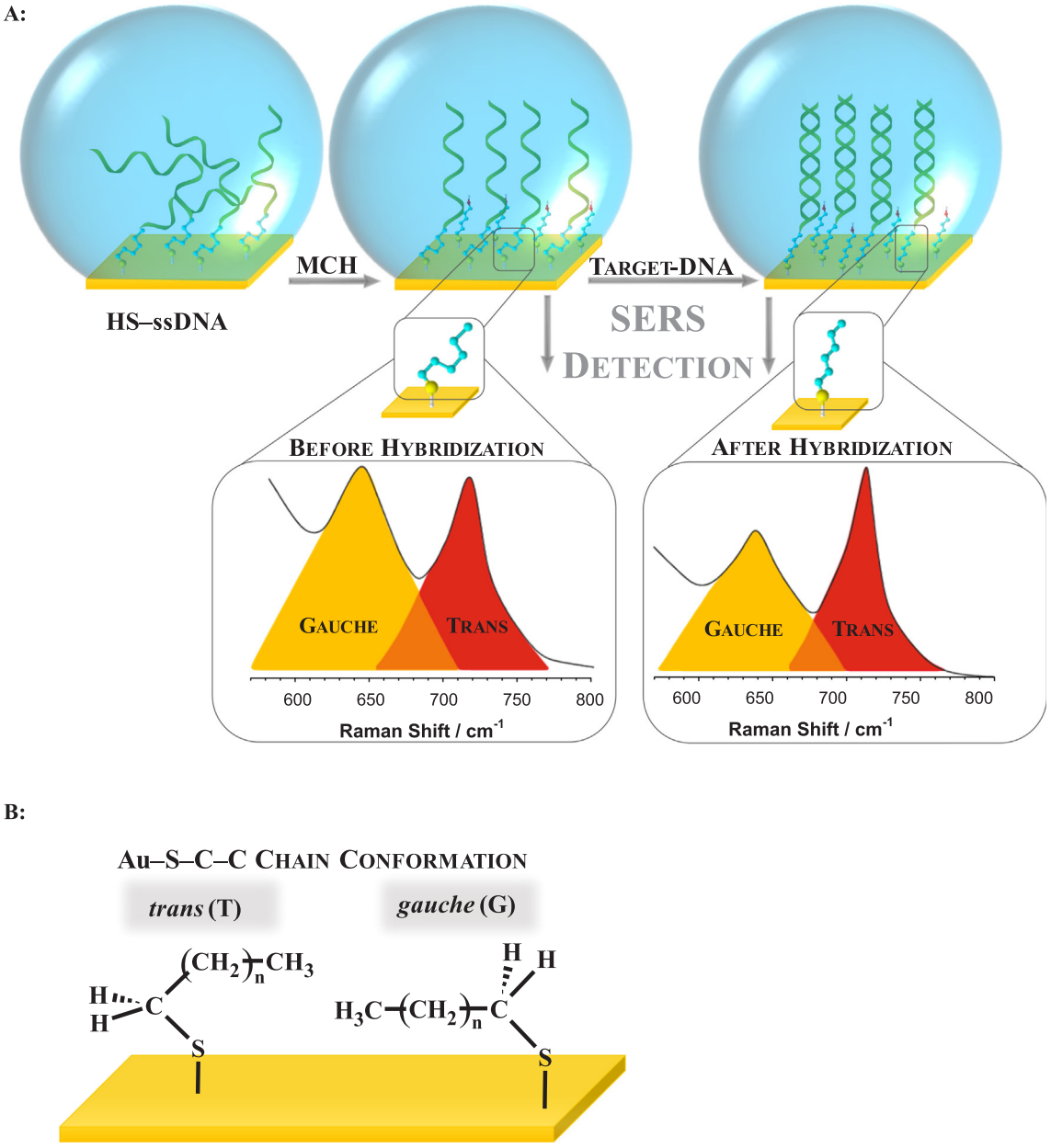

Scheme 1. A: Scheme of the procedure of modification of SERS substrates by DNA fragments. B: Possible structures of Au–S–C–C chain: *trans* (T) conformation and *gauche* (G) conformation.

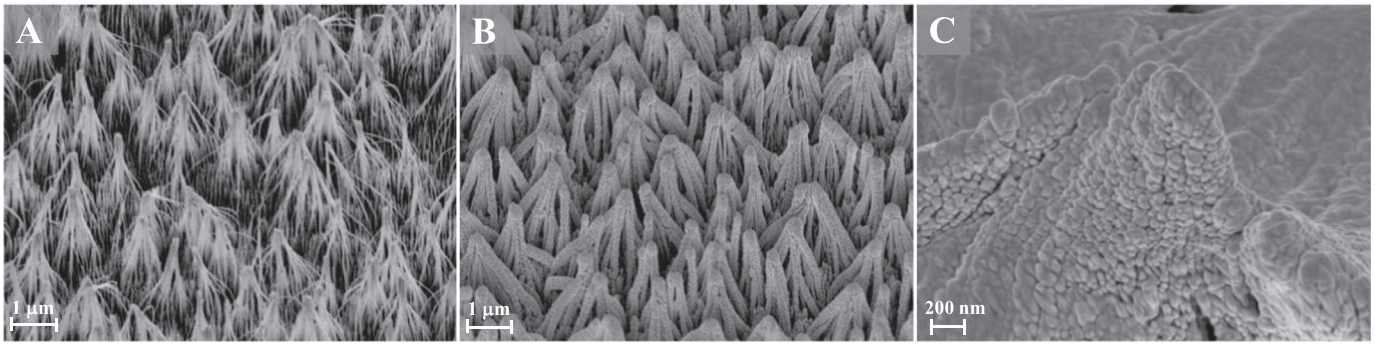

Fig. 1. SEM images of GaN samples after KSO–D photo–etching (A) and after sputtering of gold (B–C). Samples tilted 45°.

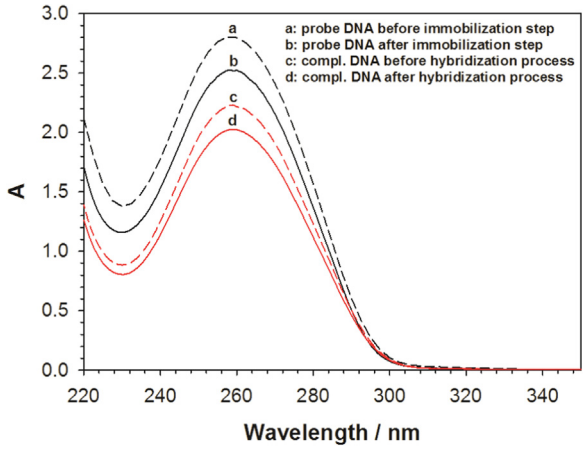

Fig. 2. UV–vis spectra of the solutions of 67.5 ng μL^{-1} probe DNA and complementary target DNA before and after interaction with 10 unmodified and probe DNA–modified SERS substrates.

with gene mutation (*BRAF*, c.1799T > A; p.600E; black lines in Fig. 3A) the relative surface concentration of the hexanethiol moieties having the *trans* conformation of the Au–S–C–C chain significantly increases (the average intensity ratio of the ν(C–S) bands of the *trans* and *gauche* conformer reaches the value above 1). When a non–complementary DNA fragments were applied, the hybridization process did not take place. Therefore, no DNA duplex can be formed and no *gauche–trans* conformation changes can be detected, see Fig. 3C. The spectra presented in Fig. 3 are the average from 20 spectra measured at various areas of the SERS substrate, however, even in a single experiment carried at a randomly chosen area of the SERS substrate the effect of the increase in the intensity ratio of the ν(C–S) bands of the *trans* and *gauche* conformer can be clearly observed. Increasing of the relative surface concentration of the thiolate moieties in *trans* conformation is typical for the process of increasing of the arrangement of the formed thiolate monolayer (Kudelski and Hill, 1999). For some systems we carried out measurements of 400 SERS spectra at different areas of the sample; the repeatability was very good; the relative standard deviation was approx. < 1% and 6.5% before and after hybridization process, respectively. The result of this experiment also shown that the used SERS substrates are very homogeneous.

The proposed biosensor was tested in the concentration range of the complementary DNA targets from 0.68 pg μL^{-1} to 0.37 μg μL^{-1}. With the increasing concentration of the analyte (target DNA) at the probe DNA–modified SERS substrate surface the increase of the intensity ratio of the ν(C–S) bands of the *trans* and *gauche* conformer is observed. Fig. 4 illustrates the obtained dependence $I_{trans}/I_{gauche} = f(C_{target\ ssDNA})$, which was linear in the DNA concentration range from 6.75 pg μL^{-1} to 67.5 ng μL^{-1}. The detection limit (LOD) was determined from the low concentration linearity range of the calibration curve according to the equation:

$$LOD = \frac{3\sigma}{a} \quad (1)$$

where σ is the standard deviation of the response of the blank (I_{trans}/I_{gauche} for GaN substrate modified with thiolated probe ssDNA before hybridization process) and *a* is the slope of the calibration curve. The determined limit of detection (LOD) was *ca.* 0.17 pg μL^{-1}.

3.3. *BRAF c.1799T > A (p.V600E) mutation SERS identification*

We decided to verify whether the process of the rearrangement of the structure of the linkage moiety *via* which the probe ssDNA is attached to the metal surface may be used as an indicator of the hybridization, and hence, may be used as a principle of operation of the SERS clinical sensors for detection of a circulating tumor DNA fragments. To carry out this experiment we used 17 various clinical samples: 10 samples from patients having *BRAF* mutation, it means containing ssDNA complementary to capture ssDNA (nine samples were

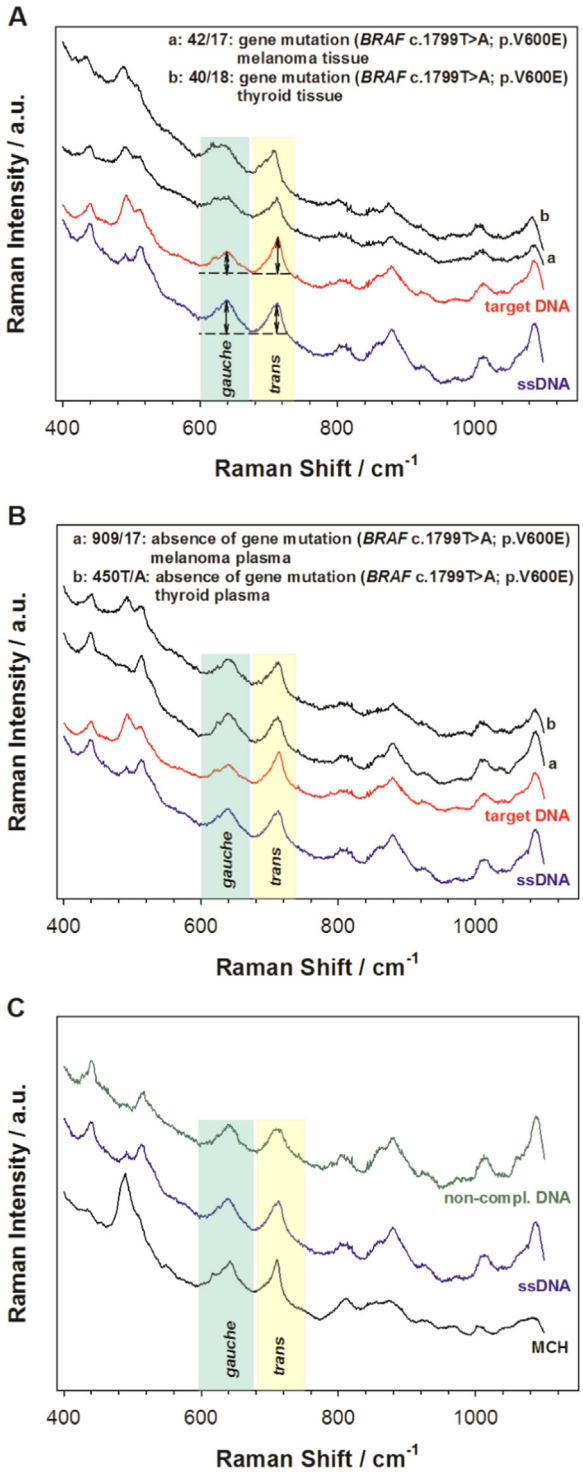

Fig. 3. SERS spectra of gold–covered nanostructured GaN substrates modified with ssDNA (blue lines) after interaction with DNA isolated from FFPE tumor tissue with detected mutation (*BRAF*, c.1799T > A; p.600E) (A), DNA isolated from plasma patients without detected mutation (*BRAF*, c.1799T > A; p.600E) (B) and non–complementary synthetic DNA (C). Red lines: fully complementary target DNA (synthetic); black lines: clinical samples; green line: non–complementary DNA (synthetic). (For interpretation of the references to color in this figure legend, the reader is referred to the web version of this article).

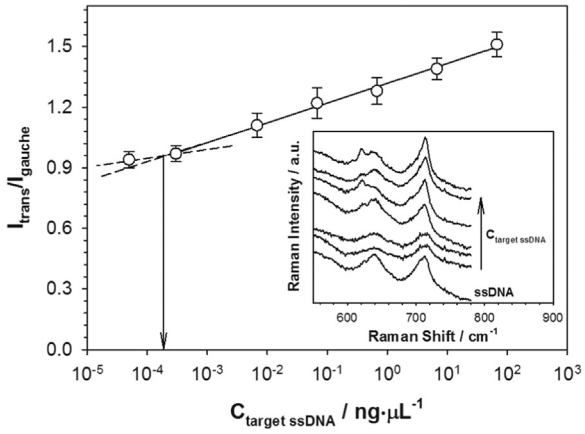

Fig. 4. Calibration plot based on SERS data. Inset: Exemplary SERS spectra of gold–covered nanostructured GaN substrates modified with ssDNA after hybridization with fully complementary synthetic target DNA in various concentration.

Table 1
Results of genotyping by ddPCR and I_{trans}/I_{gauche} ratios at gold covered nanostructured GaN substrates modified with ssDNA before and after hybridization with fully complementary target DNA (dsDNA) and clinical samples genotyped by ddPCR.

Sample	ddPCR	I_{trans}/I_{gauche}
ssDNA	synthetic	0.94
target ssDNA	synthetic	1.54
BRAF Thyroid (tissue)		
40/18	mutation p.V600E	1.13
5242/17	no mutation	0.96
BRAF Thyroid (plasma)		
450 T/A	no mutation	0.93
86 T/A	no mutation	0.91
BRAF Melanoma (tissue)		
1368/16	mutation p.V600E	1.56
2841/16	mutation p.V600E	1.09
2292/16	mutation p.V600E	1.18
42/17	mutation p.V600E	1.13
3185/17	mutation p.V600E	1.15
5526/17	no mutation	0.90
4442/17	mutation p.V600E	1.09
4647/17	mutation p.V600E	1.04
4770/17	no mutation	0.85
BRAF Melanoma (plasma)		
147/17	mutation p.V600E	1.26
4894/17	mutation p.V600E	1.13
909/17	no mutation	0.90
186/18	no mutation	0.96

from patients with melanoma and one sample was from patient with thyroid cancer) and 7 samples from patients without *BRAF* mutation. As can be seen from Table 1, when the clinical sample contained ssDNA complementary to the capture ssDNA, the intensity ratio of the ν(C–S) bands of the *trans* and *gauche* conformer was equal to at least 1.04, whereas for samples that did not contain ssDNA complementary to the capture ssDNA, this ratio was equal to maximum 0.96. It means that the observed by us process of the rearrangement of the structure of the linkage moiety *via* which the capture ssDNA is attached to the metal surface may be used as the indicator of the hybridization. Hence, the determination of this process using SERS spectroscopy may be used as a principle of the operation of the DNA SERS sensors. The SERS results were in perfect agreement with the results obtained by applying ddPCR for clinical samples genotyping.

4. Conclusions

Proposed approach provides fundamental insight into SERS detection of circulating tumor DNA fragments characteristic for *BRAF* mutation (c.1799T > A). The detection was based on the conformation changes (*trans* and *gauche*) of the thiol linker *via* which the capture ssDNA was anchored to the gold surface, caused by the hybridization process. These changes are directly associated with the amount of the double stranded DNA at gold–covered nanostructured GaN substrates. To our best knowledge the conformational changes of thiol linker in the DNA identification were used for the first time. The demonstrated new DNA SERS (bio)sensor is characterized by the low detection limit at the level of pg·μL^{-1}, wide analytical range from 6.75 pg μL^{-1} to 67.5 ng μL^{-1} and high selectivity. The most prominent achievement of this work is that the proposed bioactive platforms, based on nanostructured GaN substrates modified with thiolated ssDNA can be successfully used in the analysis of clinical samples. The constructed DNA SERS sensor has been tested on 17 clinical samples (on 10 samples from patients having *BRAF* mutation: nine with melanoma and one with thyroid cancer, and on 7 samples from patients without *BRAF* mutation). We believe that this simple approach has a great potential in medical diagnostics.

CRediT authorship contribution statement

Agata Kowalczyk: Investigation, Writing - original draft, Writing - review & editing. **Jan Krajczewski:** Investigation. **Artur Kowalik:** Resources, Writing - original draft, Writing - review & editing. **Jan L. Weyher:** Conceptualization, Investigation, Writing - original draft, Funding acquisition. **Igor Dzięcielewski:** Investigation. **Małgorzata Chłopek:** Investigation. **Stanisław Góźdź:** Conceptualization. **Anna M. Nowicka:** Conceptualization, Methodology, Writing - original draft, Writing - review & editing, Supervision. **Andrzej Kudelski:** Conceptualization, Writing - original draft, Writing - review & editing, Funding acquisition.

Acknowledgments

This work was supported by the National Science Centre of Poland Grant no. 2015/19/B/ST8/02004. Andrzej Kudelski thanks the Faculty of Chemistry, University of Warsaw for its financial support.

Ethics statement

All of the study procedures were approved local Bioethics Commission (No. 16/2014) at Jan Kochanowski University in Kielce and performed according to the Declaration of Helsinki. All patients provided signed, informed consent before enrolling in the study.

Notes

The authors declare no competing financial interest.

Declaration of interest statement

Statement 1: The manuscript, or its contents in some other form, has not been published previously by any of the authors and/or is not under consideration for publication in another journal at the time of submission.

Statement 2: All authors have seen and approved the submission of the manuscript.

Statement 3: All of the sources of funding for the work described in this publication are acknowledged.

On behalf of all co-authors

Anna M. Nowicka

References

Bettegowda, C., Sausen, M., Leary, R.J., Kinde, I., Wang, Y., Agrawal, N., Bartlett, B.R., Wang, H., Luber, B., Alani, R.M., Antonarakis, E.S., Azad, N.S., Bardelli, A., Brem, H., Cameron, J.L., Lee, C.C., Fecher, L.A., Gallia, G.L., Gibbs, P., Le, D., Giuntoli, R.L., Goggins, M., Hogarty, M.D., Holdhoff, M., Hong, S.-M., Jiao, Y., Juhl, H.H., Kim, J.J., Siravegna, G., Laheru, D.A., Lauricella, C., Lim, M., Lipson, E.J., Nagahashi Marie, S.K., Netto, G.J., Oliner, K.S., Olivi, A., Olsson, L., Riggins, G.J., Sartore-Bianchi, A., Schmidt, K., Shih, I.-M., Oba-Shinjo, S.M., Siena, S., Theodorescu, D., Tie, J., Harkins, T.T., Veronese, S., Wang, T.-L., Weingart, J.D., Wolfgang, Ch.L., Wood, L.D., Xing, D., Hruban, R.H., Wu, J., Allen, P.J., Max Schmidt, C., Choti, M.A., Velculescu, V.E., Kinzler, K.W., Vogelstein, B., Papadopoulos, N., Diaz Jr, L.A., 2014. Sci. Transl. Med. 6 (224) (224ra24).

Bryant, M.A., Pemberton, J.E., 1991a. J. Am. Chem. Soc. 113, 3629–3637.

Bryant, M.A., Pemberton, J.E., 1991b. J. Am. Chem. Soc. 113, 8284–8293.

Cao, Y.C., Jin, R., Mirkin, C.A., 2002. Science 297, 1536–1540.

Chen, L.X., Fu, X.L., Li, J.H., 2013. Nanoscale 5, 5905–5911.

Chen, K., Wu, L., Jiang, X., Lu, Z., Han, H., 2014. Biosens. Bioelectron. 62, 196–200.

Chertow, D.S., 2018. Science 360, 381–382.

Chinen, A.B., Guan, C.M., Ferrer, J.R., Barnaby, S.N., Merkel, T.J., Mirkin, C.A., 2015. Chem. Rev. 115, 10530–10574.

Crowley, E., Di Nicolantonio, F., Loupakis, F., Bardelli, A., 2013. Nat. Rev. Clin. Oncol. 10 (8), 472–484.

Davies, H., Bignell, G.R., Cox, C., Stephens, P., Edkins, S., Clegg, S., Teague, J., Woffendin, H., Garnett, M.J., Bottomley, W., Davis, N., Dicks, E., Ewing, R., Floyd, Y., Gray, K., Hall, S., Hawes, R., Hughes, J., Kosmidou, V., Menzies, A., Mould, C., Parker, A., Stevens, C., Watt, S., Hooper, S., Wilson, R., Jayatilake, H., Gusterson, B.A., Cooper, C., Shipley, J., Hargrave, D., Pritchard-Jones, K., Maitland, N., Chenevix-Trench, G., Riggins, G.J., Bigner, D.D., Palmieri, G., Cossu, A., Flanagan, A., Nicholson, A., Ho, J.W., Leung, S.Y., Yuen, S.T., Weber, B.L., Seigler, H.F., Darrow, T.L., Paterson, H., Marais, R., Marshall, C.J., Wooster, R., Stratton, M.R., Futreal, P.A., 2002. Nature 417 (6892), 949–954.

Diehl, F., Li, M., Dressman, D., He, Y., Shen, D., Szabo, S., Diaz Jr, L.A., Goodman, S.N., David, K.A., Juhl, H., Kinzler, K.W., Vogelstein, B., 2005. Proc. Natl. Acad. Sci. USA 102 (45), 16368–16373.

Domagała, P., Kowalik, A., 2014. Pol. J. Pathol. 65 (4 Suppl. 1), S59–S77.

Fabris, L., Dante, M., Braun, G., Lee, S.J., Reich, N.O., Moskovits, M., Nguyen, T.-Q., Bazan, G.C., 2007. J. Am. Chem. Soc. 129, 6086–6087.

Fu, X., Cheng, Z., Yu, J., Choo, P., Chen, L., Choo, J., 2016. Biosens. Bioelectron. 78, 530–553.

Gao, F., Lei, J., Ju, H., 2013. Anal. Chem. 85, 11788–11793.

Han, X., Wang, J., Sun, Y., 2017. Proteom. Bioinforma. 15, 59–72.

Heath, J.R., 2015. Proc. Natl. Acad. Sci. USA 112 (47), 14436–14443.

Hodis, E., Watson, I.R., Kryukov, G.V., Arold, S.T., Imielinski, M., Theurillat, J.P., Nickerson, E., Auclair, D., Li, L., Place, C., Dicara, D., Ramos, A.H., Lawrence, M.S., Cibulskis, K., Sivachenko, A., Voet, D., Saksena, G., Stransky, N., Onofrio, R.C., Winckler, W., Ardlie, K., Wagle, N., Wargo, J., Chong, K., Morton, D.L., Stemke-Hale, K., Chen, G., Noble, M., Meyerson, M., Ladbury, J.E., Davies, M.A., Gershenwald, J.E., Wagner, S.N., Hoon, D.S., Schadendorf, D., Lander, E.S., Gabriel, S.B., Getz, G., Garraway, L.A., Chin, L., 2012. Cell 150 (2), 251–263.

Huang, S., Hu, J., Zhu, G., Zhang, C., 2015. Biosens. Bioelectron. 65, 191–197.

Jabir, N.R., Tabrez, S., Ashraf, G.M., Shakil, S., Damanhouri, G.A., Kamal, M.A., 2012. Int. J. Nanomed. 7, 4391–4408.

Kaminska, A., Dzięcielewski, I., Weyher, J.L., Waluk, J., Gawinkowski, S., Sashuk, V., Fiałkowski, M., Sawicka, M., Suski, T., Porowski, S., Hołyst, R., 2011. J. Mater. Chem. 21, 8662–8669.

Kennedy, B.J., Spaeth, S., Dickey, M., Carron, K.T., 1999. J. Phys. Chem. B 103, 3640–3646.

Khetrapal, P., Liang Lee, M.W., Shen Tan, W., Dong, L., de Winter, P., Feber, A., Kelly, J.D., 2018. Cancer Treat. Rev. 66, 56–63.

Kowalik, A., Kowalska, A., Walczyk, A., Chodurska, R., Kopczyński, J., Chrapek, M., Wypiórkiewicz, E., Chłopek, M., Pięciak, L., Gąsior-Perczak, D., Pałyga, I., Gruszczyński, K., Nowak, E., Góźdź, S., 2017. PLoS One 12 (6), e0179691 (1-12).

Kudelski, A., 2003. J. Raman Spectrosc. 34, 853–862.

Kudelski, A., Hill, W., 1999. Langmuir 15, 3162–3168.

Lai, Y., Wang, J., He, T., Sun, S., 2014. Anal. Lett. 47, 833–842.

Leary, R.J., Sausen, M., Kinde, I., Papadopoulos, N., Carpten, J.D., Craig, D., O'Shaughnessy, J., Kinzler, K.W., Parmigiani, G., Vogelstein, B., Diaz Jr, L.A., Velculescu, V.E., 2012. Sci. Transl. Med. 4 (162) (162ra154).

Levicky, R., Herne, T.M., Tarlov, M.J., Satija, S.K., 1998. J. Am. Chem. Soc. 120, 9787–9792.

Morla-Folch, J., Gisbert-Quilis, P., Masetti, M., Garcia-Rico, E., Alvarez-Puebla, R.A., Guerrini, L., 2017. Angew. Chem. Int. Ed. 56, 2381–2385.

Mouliere, F., Robert, B., Arnau Peyrotte, E., Del Rio, M., Ychou, M., Molina, F., Gongora, C., Thierry, A.R., 2011. PLoS One 6 (9), e23418.

Oellerich, M., Schutz, E., Beck, J., Kanzow, P., Plowman, P.N., Weiss, G.J., Walson, P.D., 2017. Crit. Rev. Clin. Lab. Sci. 54 (3), 205–218.

Pantel, K., Alix-Panabieres, C., Riethdorf, S., 2009. Nat. Rev. Clin. Oncol. 6 (6), 339–351.

Peng, F., Su, Y., Zhong, Y., Fan, C., Lee, S.-T., He, Y., 2014. Acc. Chem. Res. 47612–47623.

Pérez-Barrios, C., Nieto-Alcolado, I., Torrente, M., Jiménez-Sánchez, C., Calvo, V., Gutierrez-Sanz, L., Palka, M., Donoso-Navarro, E., Provencio, M., Romero, A., 2016. Transl. Lung Cancer Res. 5 (6), 665–672.

Rutkowski, P., Gos, A., Jurkowska, M., Switaj, T., Dziewirski, W., Zdzienicki, M., Ptaszyński, K., Michej, W., Tysarowski, A., Siedlecki, J.A., 2014. Oncol. Lett. 8 (1), 47–54.

Schwarzenbach, H., Hoon, D.S., Pantel, K., 2011. Nat. Rev. Cancer 11 (6), 426–437.

Stiles, P.L., Dieringer, J.A., Shah, N.C., van Duyne, R.P., 2008. Annu. Rev. Anal. Chem. 1, 601–626.

Tarabara, V.V., Nabiev, I.R., Feofanov, A.V., 1998. Langmuir 14 (5), 1092–1098.

Torre, L.A., Bray, F., Siegel, R.L., Ferlay, J., Lortet-Tieulent, J., Jemal, A., 2015. CA Cancer J. Clin. 65 (2), 87–108.

van Dorp, D.H., Weyher, J.L., Kooijman, M.R., Kelly, J.J., 2009. J. Electrochem. Soc. 156, D371–D376.

Vo-Dinh, T., Allain, L.R., Stokes, D.L., 2002. J. Raman Spectrosc. 33, 511–516.

Wang, H.-N., Vo-Dinh, T.V., 2009. Nanotechnology 20, 065101.

Wang, G., Wang, Y., Chen, L., Choo, J., 2010. Biosens. Bioelectron. 25, 1859–1868.

Wang, Y., Yan, B., Chen, L., 2013a. Chem. Rev. 113, 1391–1428.

Wang, H.-N., Dhawan, A., Du, Y., Batchelor, D., Leonard, D.N., Misrad, V., Vo-Dinh, T., 2013b. Phys. Chem. Chem. Phys. 15, 6008–6015.

Wang, X., Choi, N., Cheng, Z., Ko, J., Chen, L., Choo, J., 2017. Anal. Chem. 89, 1163–1169.

Weyher, J.L., Tichelaar, F.D., Zandbergen, H.W., Macht, L., Hageman, P.R., 2001. J. Appl. Phys. 90, 6105–6109.

Weyher, J.L., Tichelaar, F.D., van Dorp, D.H., Kelly, J.J., Khachapuridze, A., 2002. J. Cryst. Growth 312, 2607–2610.

Weyher, J.L., Macht, L., 2004. Eur. Phys. J. Appl. Phys. 27, 37–41.

Weyher, J.L., Bartosewicz, B., Dzięcielewski, I., Krajczewski, J., Jankiewicz, B., Nowak, G., Kudelski, A., 2019. Appl. Surf. Sci. 466, 554–561.

Wu, X., Luo, L., Yang, S., Ma, X., Li, Y., Dong, C., Tian, Y., Zhang, L., Shen, Z., Wu, A., 2015. ACS Appl. Mater. Interfaces 7, 9965–9971.

Xu, L.-J., Lei, Z.-C., Li, J., Zong, C., Yang, C.J., Ren, B., 2015. J. Am. Chem. Soc. 137, 5149–5154.

Xu, X., Ma, X., Wang, H., Wang, Z., 2018. Microchim. Acta 185, 325.

Yu, J., Jeon, J., Choi, N., Lee, J.O., Kim, Y.-P., Choo, J., 2017. Sens. Actuators B Chem. 251, 302–309.

Zhang, Y.J., Zeng, Q.Y., Li, L.F., Qi, M.N., Qi, Q.C., Li, S.X., Xu, J.F., 2018. Opt. Express 26, 33044–33056.